European Drag Reduction and Flow Control Meeting – EDRFCM 2017
April 3–6, 2017, Rome, Italy

ENERGY TRANSFER RATES IN TURBULENT CHANNELS WITH DRAG REDUCTION AT CONSTANT POWER INPUT

D. Gatti and B. Frohnapfel
Institute of Fluid Dynamics, Karlsruhe Institute of Technology, 76131 Karlsruhe, Germany

Y. Hasegawa
Institute of Insdustrial Science, University of Tokyo, 153-8585 Tokyo, Japan

A. Cimarelli
Dept. of Engineering Sciences and Methods, Università degli Studi di Modena e Reggio Emilia, 42121 Reggio Emilia, Italy

M. Quadrio
Politecnico di Milano, Milano, Italy — Mercator Fellow, Karlsruhe Institute of Technology, Karlsruhe, Germany

INTRODUCTION

In the present work we leverage the recently-proposed Constant Power Input (CPI) approach [3, 4], in which the power transferred to the flow – through pumping and imposition of control – is kept constant, to understand how turbulent drag reduction obtained via several conceptually different strategies modifies the energetic properties of channel flows. Two questions are at the root of this research: i) whether a drag-reduced turbulent flow fundamentally differs from a "natural" turbulent flow; and ii) whether similarities exist in how different control strategies modify the flow from the energetic standpoint. Both questions are important for understanding universal mechanisms related with drag reduction and for developing turbulence models for drag-reduced flows.

METHOD

Direct Numerical Simulation (DNS) of turbulent channel flows driven at Constant Power Input (CPI) have been performed at a power-based Reynolds number, kept constant across all cases, of $Re_\Pi = U_\Pi h/\nu = 6500$. This power-based value of Re corresponds, in the reference unmanipulated channel, to $Re_\tau = u_\tau h/\nu = 199.7$ and $Re_b = U_b h/\nu = 3176.8$. In the previous definitions, U_Π is the bulk velocity of a laminar flow driven by the given power Π, u_τ and U_b are respectively the friction and the bulk velocity, h the channel semi-height and ν is the kinematic viscosity of the fluid. Two active flow control strategies for turbulent skin-friction drag reduction, which require a control power input Π_c in order to be applied, have been considered, namely the spanwise-oscillating wall ([5]) and the opposition control [1]. The calculations are carried out under both Constant total Power Input (CtPI) and Constant pumping Power Input (CpPI) conditions [2]. The total power Π_t is defined as the sum of the control power Π_c and the pumping power Π_p, so that active control uses a fraction $\gamma = \Pi_c/\Pi_t$ of the total power to function while only a fraction $(1-\gamma)\Pi_t = \Pi_p$ is available for pumping. The two control strategies of the present study (figure 1) have been selected due to their very different input power requirements, yielding different values of γ. The oscillating-wall forcing requires a significant amount of energy to operate ($\gamma = 0.1$), while the opposition control, which enforces a distributed ver-

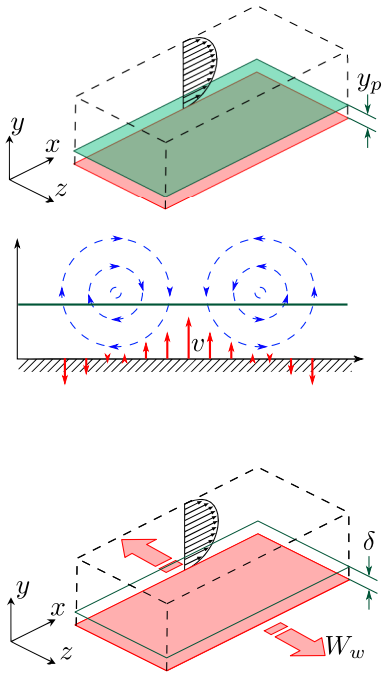

Figure 1: Sketch of the two main control strategies addressed in the present work. Top: opposition control [1] ; bottom: spanwise wall oscillations [5].

tical velocity v at the wall opposing the same component at a plane located at a prescribed wall distance y_p, requires minimal control power ($\gamma = 0.005$). The control parameters have been set in order to maximize the control performance, which in the CtPI framework means maximizing the bulk mean velocity U_b (while decreasing the wall shear stress τ_w) at a fixed total power Π_t. The ratio $U_b/U_{b,0}$ between the bulk velocity U_b in the flow with control and the one $U_{b,0}$ of the reference case is 1.028 for wall oscillations and 1.093 for opposition control. The calculations start from an initial condition where the flow has already reached statistical equilibrium for the specific controlled case, and are advanced for further 4000 time units or about 25000 viscous time units. During this time 200 flow fields are written to disk. For the two oscillating-wall cases, 200 fields are saved for each of the 8 phases, for a total of 1600 flow fields.

RESULTS

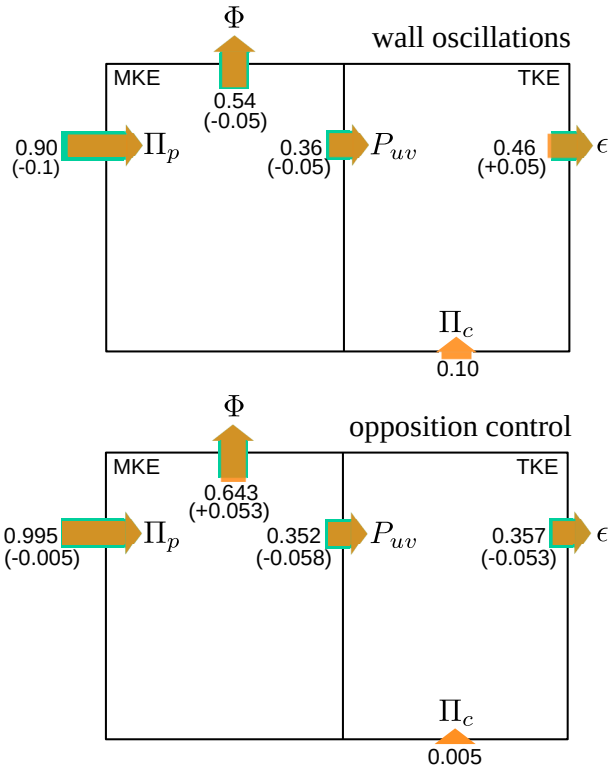

Figure 2: Energy boxes showing the integral energy transfer rates of turbulent (TKE, right) and mean (MKE, left) kinetic energy in a channel controlled under CtPI by wall oscillations (top) and opposition control (bottom). Orange colour is used for the flow with control and green colour for the reference uncontrolled flow. The values in parenthesis show the change of energy transfer rates respect to the uncontrolled flow. All values are nondimensionalized by the total power Π_t.

Figure 2 shows the time- and space-averaged transfer rates of turbulent (TKE, right) and mean (MKE, left) kinetic energy for the two control strategies considered in the present abstract, only for simulation performed under CtPI. All values are normalized by the total power input Π_t. Each box represent the turbulent channel flow as a system, which is fed with a pumping power $\Pi_p = (1-\gamma)\,\Pi_t$ and a control power $\Pi_c = \gamma\Pi_t$. The rate at which turbulence dissipates this total power input by viscous mechanisms is usually decomposed into one part Φ associated with the mean flow and another part ϵ associated with the turbulent velocity fluctuations. P_{uv} is the rate at which MKE is converted into TKE.

A first interesting information that can be extracted from the energy box representation is that the oscillating wall, which diverts about 10% – a significant fraction – of the total power from the pump to feed the control system, achieves a higher flow rate than the canonical channel flow. Given that most of Π_c is directly dissipated by the Stokes layer itself via viscosity, one observes that oscillating a wall is a successful way of disrupting turbulence which, surprisingly, is a good alternative to pumping. On the other hand, opposition control, which requires a much smaller fraction of the total available power, causes a larger increase of U_b with respect to the uncontrolled channel compared to wall oscillations.

Searching for changes of such energy transfer rates, particularly dissipation rates, that show common features across different drag reduction strategies would lead to identify universal properties of drag reduction. Surprisingly, however, figure 2 shows that both opposition control and wall oscillations achieve higher flow rate than the reference channel, but changes in energy dissipation rates have opposite signs. With wall oscillations Φ, the dissipation of MKE, is decreased compared to the reference channel while ϵ, the dissipation of TKE, is increased; with opposition control, the opposite behaviour is observed.

Despite this contrasting picture, at the meeting we will show how universal features in the changes of energy transfer related to drag reduction can be identified. Such features depend on alternative decompositions of the total dissipation rate.

Support through DFG project FR2823/5-1 is gratefully acknowledged. Computing time has been provided by the computational resource ForHLR Phase I funded by the Ministry of Science, Research and the Arts, Baden-Wrttemberg and DFG (Deutsche Forschungsgemeinschaft).

REFERENCES

[1] H. Choi, P. Moin, and J. Kim. Active turbulence control for drag reduction in wall-bounded flows. *J. Fluid Mech.*, 262:75–110, 1994.

[2] B. Frohnapfel, Y. Hasegawa, and M. Quadrio. Money versus time: evaluation of flow control in terms of energy consumption and convenience. *J. Fluid Mech.*, 700:406–418, 2012.

[3] Y. Hasegawa, M. Quadrio, and B. Frohnapfel. Numerical simulation of turbulent duct flows at constant power input. *J. Fluid Mech.*, 750:191–209, 2014.

[4] M. Quadrio, B. Frohnapfel, and Y. Hasegawa. Does the choice of the forcing term affect flow statistics in DNS of turbulent channel flow? *Eur. J. Mech. B / Fluids*, 55:286–293, 2016.

[5] M. Quadrio and P. Ricco. Critical assessment of turbulent drag reduction through spanwise wall oscillation. *J. Fluid Mech.*, 521:251–271, 2004.